JOURNAL OF MATERIALS SCIENCE 19 (1984) 923–928

Transverse tensile strength anisotropy in thick filament wound ring composites

A. MIYASE
Department of Mechanical Engineering, University of Ottawa, Ottawa, Ontario K1N 6N5, Canada

The transverse tensile strength of glass/epoxy thick filament wound ring composites depends on the size and orientation of the tensile specimens and on the winding atmospheres. The void geometries, distribution, and content are altered by the fabrication atmospheres and type of glass fibre. The dependence of strength on specimen orientation and size appears to be attributed to the existence of elongated "pancake" shaped voids between strands. The Mode I critical stress intensity factor was measured using width-tapered double cantilever beams. Some attempts were made to correlate void size with transverse strength for several specimen orientations.

1. Introduction

The transverse tensile strength of unidirectional composites is usually measured by pulling thin plates in the in-plane transverse direction. In the case of thin plates, microstructural irregularities, such as voids can be minimized without much difficulty by optimizing fabrication conditions. With increasing thickness, however, it becomes very difficult to fabricate composites with few voids. The void size, distribution, and shape may differ, depending on manufacturing methods (i.e., dry lay-up or wet lay-up). In general, voids tend to stay between plies or strands and to elongate in in-plane directions because of the ease of epoxy flow during fabrication. Consequently, transverse tensile properties of thick composites may show some differences between in-plane and out-of-plane transverse directions.

In many cases, out-of-plane transverse stress is insignificant in comparison with in-plane transverse stress. One exception is the stress condition which exists near a free edge of a laminate with a particular stacking sequence [1, 2]. However, laminates with thin cross-sections imply few voids. Consequently, little difference in strength for the two different transverse directions can be expected.

Three-dimensional elastic properties have been measured by several investigators [3, 4]. The measurments were made either mechanically or ultra-sonically on thick graphite/epoxy composites. These investigators found no modulus difference in in-plane and out-of-plane transverse directions. Out-of-plane transverse strength was reported by Nimmer *et al.* [4], where tensile specimens were cut out of a graphite/epoxy thick filament wound ring in the radial direction. However, a comparison between in-plane and out-of-plane transverse strengths was not made.

This experiment was primarily designed to investigate in-plane and out-of-plane transverse tensile strengths in a thick filament wound ring. The effects of specimen orientations, sizes and manufacturing processes on the strengths were also examined.

2. Materials and experimental procedure

Fibres employed in this investigation were 3709 E-glass and S2-glass, and matrix epoxy Epon 825 with Ancamine 1482 hardener. Thick wall ring specimens (diameter 266.7 mm, width 25.4 mm, and thickness approximately 9 mm) were fabricated by a wet filament winding process. The process was carried out in ambient and vacuum (~ 7 kPa) atmospheres. Winding tension of 25N/1000 strand tex was applied to fabricate composites with relatively high fibre volume fraction. Details of the winding technique are to be found

0022–2461/84 $03.00 + .12

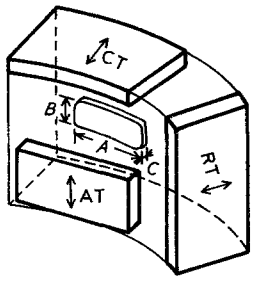

Figure 1 Transverse tensile specimen orientations from thick ring specimens (arrows indicate loading directions) and void dimensions.

elsewhere [5]. The cure cycle used was 1.5 h at 100° C and 4 h at 150° C.

Transverse tensile specimens with three different orientations were sectioned from the rings using a water-cooled diamond wheel. These were axial transverse (AT), radial transverse (RT) and circumferential transverse (CT), and are shown schematically in Fig. 1. The specimen sections were approximately 1.5 mm oversized in thickness and sanded down to the pre-determined thickness of 2 mm and width of 25 mm using emery paper. Final sanding was carried out using 600 grit emery paper to ensure a very smooth surface finish.

Sections were mounted in butt joint fashion to S2-glass/epoxy cross-ply laminate tabs using the same epoxy as adhesive. Tensile tests were carried out with a screw driven Instron universal testing machine under constant cross-head speed which produced a strain rate of between 1 and 2% per minute. A minimum of six specimens were tested for each gauge length.

Fibre volume fraction and void content were calculated from density measurements and resin burn-off methods. Composite cross-sections were also prepared metallographically and void sizes measured by a microscope with a micrometer-driven specimen stage.

3. Experimental results

The variation of transverse strength with specimen volume for three different specimen orientations in E-glass/epoxy and S2-glass/epoxy composites fabricated in two different atmospheres are shown in Figs. 2 and 3. Transverse strengths differed with specimen orientations for E-glass and S2-glass composites. The specimens oriented in the axial transverse directions were usually the strongest and showed the smallest volume dependence. On the other hand, the specimens oriented in the circumferential transverse direction were weakest and showed the strongest volume dependence. Different trends in the dependence of strength on specimen volume and orientation were found in E-glass and S2-glass composites. E-glass composites showed strong dependence on specimen volume and orientation, but S2-glass did not. Fabrication atmospheres affected the dependence of strength on specimen volume and orientation in E-glass composites. On the other hand, these effects on S2-glass composites were slight.

For the sake of clarity, no scatter bands were

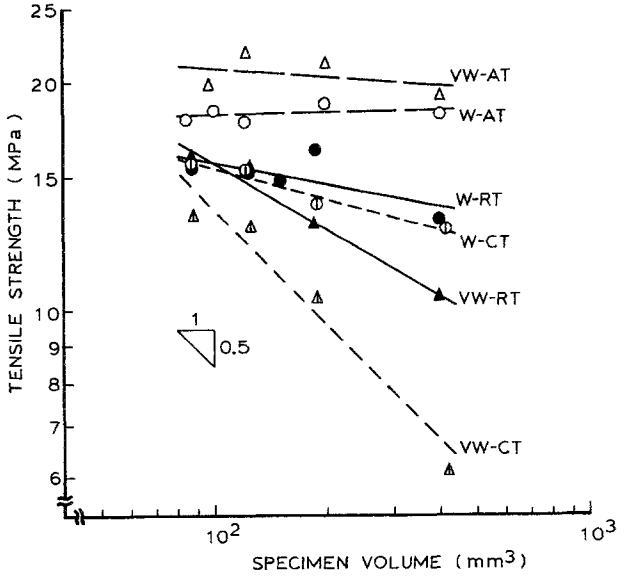

Figure 2 Variation of strength with specimen volume for three orientations in E-glass/epoxy composite in log–log scale (W: wound in an ambient atmosphere, VW: wound in a vacuum atmosphere).

TABLE I Fibre volume fraction and void content of thick ring specimens

Type of fibre	Winding atmosphere	Fibre volume fraction (%)	Void content (%)
E-Glass	Ambient	69.9	1.51
	Vacuum	70.8	0.85
S2-Glass	Ambient	63.0	3.63
	Vacuum	63.8	1.99

TABLE II Measured void dimensions

Type of fibre	Winding atmosphere	Void dimensions* (mm) *A*	*B*	*C*
E-Glass	Ambient	2.00	1.50	0.35
	Vacuum	3.20	3.00	0.12
S2-Glass	Ambient	2.00	0.15	0.12
	Vacuum	2.00	0.15	0.12

*See Fig. 1.

indicated in Figs. 2 and 3. In general, E-glass specimens showed large scatter, particularly the ones from the ring wound in vacuum. Strength scatter in S2-glass specimens from rings wound in both vacuum and ambient atmospheres were very small. No systematic variations in the scatter with specimen volume were observed for any of the different types of specimen.

Fibre volume fraction and void content of composites are shown in Table I. Fibre volume fraction was not affected by winding atmosphere; however, winding in vacuum reduced void content by a factor of approximately 2. The void distributions in radial section of E-glass rings woud in vacuum and in ambient atmosphere and of an S2-glass ring wound in a vacuum atmosphere are shown in Figs. 4, 5 and 6, respectively. Observed maximum void dimensions are shown in Table II. The void form was an elongated "pancake" shape as shown in Fig. 1.

4. Discussion

Although E- and S2-glass rings were manufactured under the same winding conditions, some differences in fibre volume fraction were observed. This could be attributed to the differences in wetting behaviour between E- and S2-glasses. The differences in void content and distribution between E- and S2-glass rings seem to support the hypothesis; however, exact mechanisms remain unknown.

The effect of ply thickness (or volume) on the onset of transverse cracking and free edge delamination were analysed by Wang and Crossman [6]. They explained the volume effects using the strain energy release rate concept because the onset stress depended inversely on the square root of the thickness of the 90° plies where the failure occurred. The size effect observed in this experiment, however, cannot be explained by the same concept. According to their theory, the slope of strength against volume plot in log–log scale should be -0.5. The observed slope in this experiment ranged from approximately zero to -0.5. The existence of rather large voids found in the specimens seemed to account for the volume and winding atmosphere dependence and anisotropy of transverse tensile strength in this experiment.

The elongated "pancake" shaped voids introduced different effective flaw sizes in tensile specimens, depending on their orientations. In the CT orientation, flaw size was largest, consequently CT specimens showed the lowest stregnth. On the other hand, in the AT orientation crack size was smallest – therefore its strength was the highest of the three specimen orientations. In E-glass/epoxy composities, lower void content did not always indicate higher strength. Although vacuum winding brought lower void content, void distribution was very localized and large voids were formed (Fig. 4). On the other hand, atmospheric

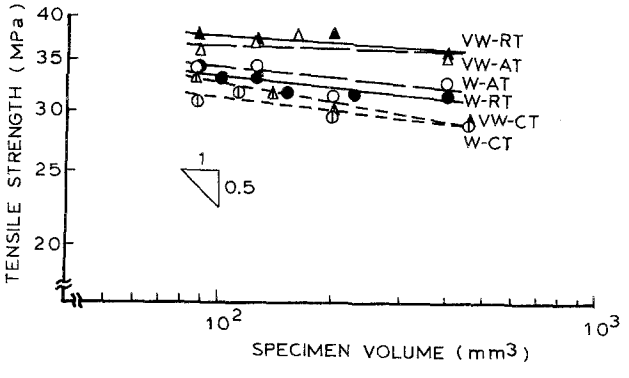

Figure 3 Variation of strength with specimen volume for three orientations in S2-glass/epoxy composite in log–log scale (W: wound in an ambient atmosphere, VW: wound in a vacuum atmosphere).

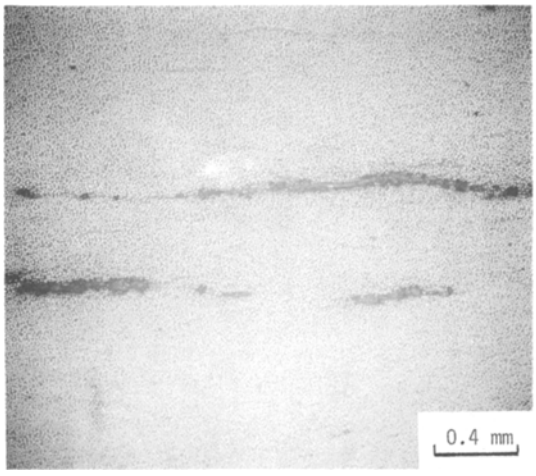

Figure 4 Void distribution in an E-glass ring wound in a vacuum atmosphere.

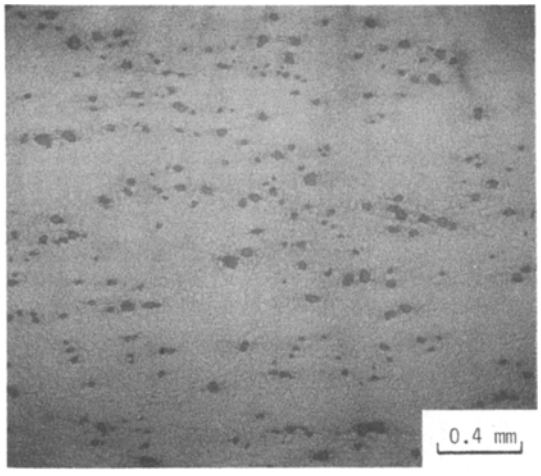

Figure 6 Void distribution in an S2-glass ring wound in a vacuum atmosphere.

winding introduced higher void content, but voids were relatively small and uniformly distributed (Fig. 5). In S2-glass/epoxy composites, both vacuum and atmospheric wound rings showed uniformly distributed voids (Fig. 6). From these observations, it seems that transverse strength anisotropy and specimen size effects are caused by differences in void content, shape, size and distribution.

In order to examine the strength anisotropy more closely, bar specimens (width 25.4 mm, thickness 13.7 mm, and length approximately 125 mm) were fabricated by the wet filament winding process. During the curing process, wound strands were cut at one end and vacuum was applied before the top plates were placed on the winding. Using this technique, composites were fabricated which were almost void free. Transverse tensile specimens were sectioned from the E-glass/epoxy bar in three different orientations, as shown in Fig. 7. The dimensions of the specimens were 2 mm thick, 25 mm wide and 11.5 mm long. Tensile tests were carried out in the same fashion as specimens from thick rings. A minimum of six specimens was tested for each orientation. The results are shown in Table III, together with fibre volume fraction and void content. No dependence of strength on specimen orientation was observed.

Some efforts were made to correlate flaw size and transverse strength of thick rings using the linear elastic fracture mechanics concept. Mode I critical strain energy release rate (G_{IC}) was measured using a Width Tapered Double Cantilever Beam (WTDCB) machined from bar specimens of E-glass/epoxy and S2-glass/epoxy. The analyses and experimental procedures of WTDCB were carried out following similar ones performed by Mostovoy *et al.* [7] and Bascom *et al.* [8]. Six WTDCB specimens were tested for each composite.

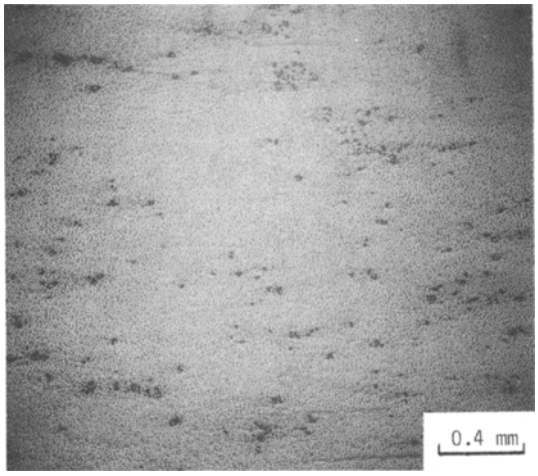

Figure 5 Void distribution in an E-glass ring wound in an ambient atmosphere.

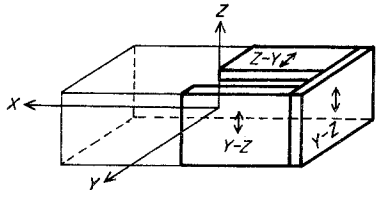

Figure 7 Transverse tensile specimen orientations from bar specimens (arrows indicate loading directions).

TABLE III Fibre volume fraction, void content and tensile test results of transverse specimens form E-glass/epoxy bar specimens

Fibre volume fraction (%)	Void content (%)	$Z-Y$		$X-Z$		$Y-Z$	
		Modulus (GPa)	Strength (MPa)	Modulus (GPa)	Strength (MPa)	Modulus (GPa)	Strength (MPa)
58.1	<0.1	20 ± 1	56 ± 3	21 ± 2	56 ± 3	19 ± 1	57 ± 6

From the obtained G_{IC}, K_{IC} was computed using the elastic coefficient for an orthotropic material in crack opening mode [9]. G_{IC} and K_{IC} values for E-glass/epoxy and S2-glass/epoxy are shown in Table IV. These values showed good agreement with published data [10–13]. Predicted transverse tensile strength can be expressed as:

$$\sigma = \frac{K_{IC}}{f(a/w)(\pi a)^{1/2}}$$

where σ = predicted strength
K_{IC} = mode I critical stress intensity factor
$f(a/w)$ = stress intensity calibration factor
a = flaw size
w = specimen width

Because of the difficulty of estimating stress intensity calibration factor, flaw lengths, and geometries, quantitative evaluations were only attempted for the through-thickness flaw configuration which was observed in some specimen orientations. Although several flaw geometries, such as central flaw, single edge, and double edge flaws with a half of measured crack length were tried, the prediction always overestimated the observed strengths. The addition of inherent characteristic flaw length, which was calculated from tensile data of bar specimens, to measured flaw lengths had little effect. The most severe case attempted was double edge flaws with a measured flaw length. Even in this case, predicted and observed strengths differed by a factor of 1.5 to 2, as shown in Table V. These discrepancies are probably caused by incorrect choice of stress intensity calibration factor, together with oversimplification of real flaw geometries. The stress intensity calibration factor which is available for this flaw configuration is for specimen length-to-width ratio of 1 [9]. With a decrease of the ratio, the calibration factor tends to increase [9]. Also, actual flaw configuration was very complex and it is highly probable that some flaws exist co-linearly. As shown in the calibration factor of two equal length co-linear flaws in an infinite sheet under uniform stress [9], co-linear flaws tend to link together because of higher stress intensity at the inner end of the flaws. If this growth-like process precedes final failure, the predictions using observed flaw sizes would result in overestimating strengths.

TABLE IV Measured G_{IC} and K_{IC} values

Type of fibre	G_{IC} ($J\,m^{-}$)	K_{IC} ($MPa\,m^{1/2}$)
E-glass	214 ± 30	2.03 ± 0.13
S2-glass	239 ± 35	2.31 ± 0.17

5. Conclusions

The existence of elongated "pancake" shaped voids appeared to be the main cause of transverse strength anisotropy and specimen size effects. The degree of anisotropy and size effect varied with total void content, void distribution, and void geometry. The linear elastic fracture mechanics approach seemed to be applicable; however, very complex void distribution and geometry made it very difficult to make correct quantitative predictions.

Acknowledgements

This research was partly supported by National Research Council of Canada Contract No. 0SU80-00043.

TABLE V Comparison of predicted strength with observed strength for several specimen orientations

Type of fibre	Winding atmosphere	Specimen orientation	Observed strength (MPa)	Predicted strength (MPa)
E-Glass	Ambient	RT	13.2	23.0
	Ambient	CT	6.3	16.4
	Vacuum	RT	10.4	16.9
S2-Glass	Ambient	RT	31.7	46.0
	Vacuum	RT	35.8	46.0

References

1. N. J. PAGANO and R. B. PIPES, *Int. J. Mech. Sci.* 15 (1973) 679.
2. F. W. CROSSMAN, W. J. WARREN, A. S. D. WANG and G. E. LOW Jr., *J. Composite Mater. Suppl.* 14 (1980) 88.
3. M. KNIGHT, *J. Composite Mater.* 16 (1982) 153.
4. R. D. NIMMER, K. TORROSIAN and W. W. WILKENING, UCRL-15383 (General Electric, Schenectady, New York, 1981).
5. M. MUNRO, A. MIYASE, J. McCREA and R. C. FLANAGAN, in Proceedings of the 17th Intersociety Energy Conversion Engineering Conference, Los Angeles, California, August 1982 (IEEE, New York, 1982) p. 1967.
6. A. S. D. WANG and F. W. CROSSMAN, *J. Composite Mater. Suppl.* 14 (1980) 71.
7. S. MOSTOVOY, P. B. CROSLEY and E. J. RIPLING, *J. Mater.* 12 (1967) 661.
8. W. D. BASCOM, J. L. BINTER, R. J. MOULTON and A. R. SIEBERT, *Composites* 11 (1980) 9.
9. P. C. PARIS and G. C. SIH, ASTM STP 381 (American Society for Testing and Materials, Philadelphia, 1965) p. 30.
10. G. C. SIH, P. D. HILTON, R. BADALIANCE, P. S. SHENBERGER and G. VILLARREAL, ASTM STP 521 (American Society for Testing and Materials, Philadelphia, 1973) p. 98.
11. J. M. SLEPETZ and L. CARLSON, ASTM STP 593 (American Society for Testing and Materials, Philadelphia, 1975) p. 143.
12. D. F. DEVITT, R. A. SCHPERY and W. L. BRADLEY, *J. Composite Mater.* 14 (1980) 270.
13. R. J. SANFORD and F. R. STONESIFER, *ibid.* 5 (1971) 241.

Received 21 March
and accepted 22 July 1983